of using it in regions with low dielectric constants and the difficulty of designing an interference-free lead wire system for the probe. An implantable electric field probe with an interference-free lead-wire system has subsequently been developed by our laboratory. This information will be published in a future paper.

References

[1] C. C. Johnson and A. W. Guy, "Nonionizing electromagnetic wave effects in biological materials and systems," *Proc. IEEE*, vol. 60, pp. 692–718, June 1972.

[2] C. C. Johnson, "Research needs for establishing a radio frequency electromagnetic radiation safety standard," *J. Microwave Power*, vol. 8, pp. 367–388, Nov. 1973.

[3] S. M Michaelson, "Review of a program to assess the effects on man from exposure to microwaves," *J. Microwave Power*, vol. 9, June 1974.

[4] H. Bassen, M. Swicord, and J. Abita, "A miniature broad-band electric field probe," *Ann. N.Y. Acad. Sci.*, vol. 247, pp. 481–493, 1975.

[5] A. Cheung, H. Bassen, M. Swicord, and D. Witters, "Experimental calibration of a miniature electric field probe within simulated muscular tissues," in *Proc. 1975 URSI Bioeffects Symp.*, to be published.

[6] G. Smith, "A comparison of electrically-short bare and insulated probes for measuring the local radio frequency electric field in biological systems," *IEEE Trans. Biomed. Eng.*, vol. ME-22, pp. 477–783, Nov. 1975.

[7] B. S. Guru and K. M. Chen, "Experimental and theoretical studies on electromagnetic fields induced inside finite biological bodies," *IEEE Trans. Microwave Theory Tech.*, vol. MTT-24, pp. 433–440, July 1976.

[8] H. Bassen, W. Herman, and R. Ross, "EM probe with fiber optic telemetry system," *Microwave J.*, pp. 35–47, Apr. 1977.

[9] H. Bassen, A. Cheung, and K. M. Chen, "Comments on 'Experimental and theoretical studies on electromagnetic fields induced inside finite biological bodies,'" *IEEE Trans. Microwave Theory Tech.*, vol. MTT-25, pp. 623–624, July 1977.

[10] R. W. P. King, "The many faces of the insulated antenna," *Proc. IEEE*, vol. 64, 228–238, Feb. 1976.

[11] J. A. Stratton and L. J. Chu, "Forced oscillation of a conducting sphere," *J. Appl. Phys.*, vol. 12, pp. 230–248, Mar. 1941.

[12] M. Abramowitz and I. A. Stegun, *Handbook of Mathematical Functions*. New York: Dover, 1970.

[13] L. Infeld, "The influence of the width of the gap upon the theory of antennas," *Quart. Appl. Math.*, vol. V, pp. 113–132, July 1947.

[14] S. H. Mousavinezhad, "Implantable electromagnetic field probes in finite biological bodies," Michigan State Univ., East Lansing, Ph.D. disertation, 1977.

[15] H. Mousavinezhad, K. M. Chen, and D. P. Nyquist, "Implantable field probes in finite biological bodies," presented at the 1976 Int. IEEE/AP-S Symp., Univ. of Massachusetts, Amherst, Oct. 1976.

[16] D. Livesay and K. M. Chen, "EM field induced inside arbitrarily-shaped biological bodies," *IEEE Trans Microwave Theory Tech.*, vol. MTT-22, pp. 1273–1280, Dec. 1974.

Heat Potential Distribution in an Inhomogeneous Spherical Model of a Cranial Structure Exposed to Microwaves Due to Loop or Dipole Antennas

ALTUNKAN HIZAL AND YAHYA KEMAL BAYKAL

Abstract—**An inhomogeneous spherical model of a 3.3-cm radius cranial structure is assumed to be placed symmetrically in the near field of a small loop antenna or an electrical dipole antenna at 3 GHz. The transitions between the layers are taken to be sharp but sinusoidal. Calculations of the heat potential are performed using a spherical wave expansion technique in which linear differential equations are solved for the unknown multipole coefficients. The results are also compared with the plane-wave excitations. It is seen that a more uniform distribution of the heat potential occurs for the dipole antenna excitation which is also similar to the *E*-plane distribution in the case of plane-wave excitation. For the loop excitation, a significant hot spot occurs near the center of the structure.**

Manuscript received July 8, 1977; revised February 21, 1978.

A Hizal is with the Electrical Engineering Department, Middle East Technical University, Ankara, Turkey.

Y. K. Baykal was with the Electrical Engineering Department, Middle East Technical University, Ankara, Turkey. He is now at Northwestern University, Evanston, IL 60201.

I. Introduction

THE PREDICTION of the heat potential distribution in a cranial structure excited by a microwave radiation is of interest for the purposes of medical treatment and searching out the radiation hazards. For this purpose, multilayered spherical models [1], [2] irradiated by a plane wave have been analyzed. It is found that a nonuniform

0018-9480/78/0800-0607$00.75

heat potential distribution, which gives rise to the "hot-spots" in the structure, occurs mostly in the resonance region where the radius of the structure ranges from about 6 to 16 percent of the free-space wavelength [2].

Previous investigations are based mostly on the assumption of a plane-wave incidence. It might be of interest also to study the heat potential distribution for sources other than a plane wave. In this connection, Guy [3] has analyzed layered biological tissues exposed to radiation from a rectangular aperture. The results indicated that the heating of the tissues exceeds that produced by a plane wave. Ho [4] has presented results for the dose rate distributions with the unit mass density, which is equivalent to the heat potential, for five layered monkey heads of 3.3 cm at 2.45 GHz for a TE_{10} contact aperture source. The results indicate that the aperture source predominantly yields absorption on the surface, and microwave energy penetration into the central region is weak. In the present investigation, small loop or dipole antennas are considered as the sources of radiation which excite an inhomogeneous spherical model of a cranial structure situated symmetrically in the near zone of these antennas.

The idealized model chosen is the six-layered spherical model with a maximum radius of 3.3 cm which might correspond to a monkey's or an infant's heat. The outer five layers make up the inhomogeneous medium, the brain being the homogeneous core. The frequency is chosen to be 3 GHz at which peak internal heat potential makes a maximum for the plane-wave excitation [2]. The permittivity and the conductivity of the layers are taken at this specific frequency with sharp sinusoidal transitions between the layers. The choice of a continuously inhomogeneous model allows one to study the effect of these boundaries on the heat potential distribution. The current distribution on the infinitesimally thin loop and dipole antennas are assumed to be constant and sinusoidal, respectively.

II. Formulation of the Problem

The scattering problem cited in Fig. 1 is solved by the state-space method [5] after having it extended to the case with a homogeneous dielectric inner core.

1) For the electrical loop excitation, the incident electric field for $r<(a^2+d^2)^{1/2}$ may be expressed by the $m=0$ terms of the spherical vector harmonics expansion as

$$E_\phi^i(r,\theta)=Z_0\sum_{n=1}^{\infty} c_n\beta_n^i j_n(kr)\frac{d}{d\theta}P_n \tag{1}$$

where $c_n=\{(2n+1)/[4\pi n(n+1)]\}^{1/2}$, $j_n(kr)$ is the spherical Bessel function with $k=2\pi/\lambda$ being the wavenumber in free space, $P_n=P_n(\cos\theta)$ is the Legendre function, and r, θ, ϕ are the spherical coordinates. $Z_0=(\mu_0/\epsilon_0)^{1/2}=120\pi$ ohms is the intrinsic impedance of the free space. The multipole coefficient β_n^i is given by

$$\beta_n^i=-ak^2I_0 2\pi c_n h_n^{(1)}\left[k(a^2+d^2)^{1/2}\right]\frac{d}{d\theta_s}P_n \tag{2}$$

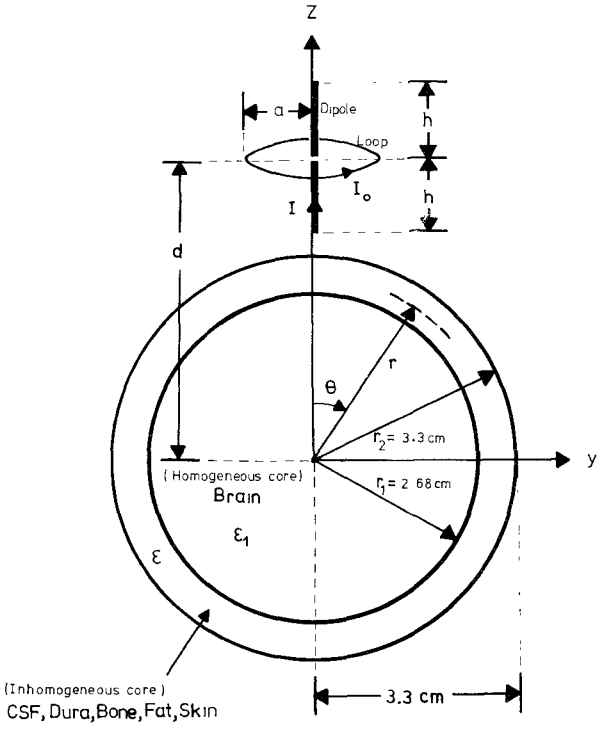

Fig. 1. Geometry of the problem for loop or dipole antenna excitations.

where I_0 is the current in amps, $h_n^{(1)}(kr)$ is the spherical Hankel function, and $\theta_s=\tan^{-1}(a/d)$. The scattered electric field in the inhomogeneous dielectric layer for $r_1\leqslant r\leqslant r_2$ for $\exp(-j\omega t)$ time dependence is expressed by

$$E_\phi^{sc}(r,\theta)=Z_0\sum_{n=1}^{\infty} c_n \cdot\left[\beta_n^1(kr)j_n(kr)+\beta_n^s(kr)h_n^{(1)}(kr)\right]\frac{d}{d\theta}P_n \tag{3}$$

where the multipole coefficients satisfy the first-order coupled linear differential equations (state equations) for $\beta_n^1(kr)+\beta_n^i$ and $\beta_n^s(kr)$ given in [5]. The unknown multipole coefficients are found by solving these differential equations subject to the boundary conditions

$$\beta_n^s(kr_1)=F_n(k_1r_1)\left[\beta_n^1(kr_1)+\beta_n^i\right] \tag{4}$$

$$\beta_n^1(kr_2)=0. \tag{5}$$

Here, $F_n(k_1r_1)$ is the Mie scattering function [6] given by

$$F_n(k_1r_1)=jkr_1j_n(kr_1)T_n/\left[j_n(k_1r_1)-jkr_1h_n^{(1)}(kr_1)T_n\right] \tag{6}$$

$$T_n=\left[r_1j_n(kr_1)\right]'j_n(k_1r_1)-j_n(kr_1)\left[r_1j_n(k_1r_1)\right] \tag{7}$$

where the prime indicates the derivative with respect to r_1, $k_1=k(\epsilon_1)^{1/2}$, and $\epsilon_1=\epsilon_{r1}+j\sigma_1/(\omega\epsilon_0)$ is the complex dielectric constant of the homogeneous inner core.

The total field in the homogeneous inner core for $0\leqslant r\leqslant r_1$ is given by

$$E_\phi^c(r,\theta)=Z_0(\epsilon_1)^{-1/2}\sum_{n=1}^{\infty} c_n\beta_n^c j_n(k_1r)\frac{d}{d\theta}P_n \tag{8}$$

where the multipole coefficient β_n^c is obtained from $E_\phi^c(r_1,\theta)=E_\phi^i(r_1,\theta)+E_\phi^{sc}(r_1,\theta)$ and the orthogonality of the Legendre's functions on a spherical surface. It can easily be shown that

$$\beta_n^c=(\epsilon_1)^{1/2}\{[\beta_n^1(kr_1)+\beta_n^i]j_n(kr_1)+\beta_n^s(kr_1)h_n^{(1)}(kr_1)\}/j_n(k_1r_1). \quad (9)$$

The heat potential is given by $P_h=(1/2)\sigma|E_\phi|^2$, where E_ϕ is the total electric field in the dielectric and is given by $E_\phi=E_\phi^i+E_\phi^{sc}$, (1) and (3) for the inhomogeneous layer and $E_\phi=E_\phi^c$, and (8) for the homogeneous inner core.

2) For the electric dipole excitation, the incident electric field for $r<(d-h)$ may be expressed by the $m=0$ terms of the vector spherical harmonics expansion as

$$E_r^i(r,\theta)=-Z_0\sum_{n=1}^{\infty}n(n+1)c_n\alpha_n^i j_n(kr)\frac{1}{kr}P_n \quad (10)$$

$$E_\theta^i(r,\theta)=-Z_0\sum_{n=1}^{\infty}c_n\alpha_n^i[rj_n(kr)]'\frac{1}{kr}\frac{d}{d\theta}P_n \quad (11)$$

where the multipole coefficient α_n^i is given by

$$\alpha_n^i=kI_0c_n\{k(d-h)h_n^{(1)}[k(d-h)]+k(d+h)h_n^{(1)}\cdot[k(d+h)]-2kdh_n^{(1)}(kd)\cos kh\} \quad (12)$$

for the sinusoidal current distribution $I(r)=I_0\sin[k(h-|r-d|)]$. The scattered electric field in a vacuum gap of vanishingly small thickness at r in the inhomogeneous dielectric layer for $r_1\leqslant r\leqslant r_2$ is expressed by

$$E_r^{sc}(r,\theta)=-Z_0\sum_{n=1}^{\infty}n(n+1)c_n\cdot[\alpha_n^1(kr)j_n(kr)+\alpha_n^s(kr)h_n^{(1)}(kr)]\frac{1}{kr}P_n \quad (13)$$

$$E_\theta^{sc}(r,\theta)=-Z_0\sum_{n=1}^{\infty}c_n\{\alpha_n^1(kr)[rj_n(kr)]'+\alpha_n^s(kr)[rh_n^{(1)}(kr)]'\}\frac{1}{kr}\frac{d}{d\theta}P_n \quad (14)$$

where the multipole coefficients $\alpha_n^1(kr)$ and $\alpha_n^s(kr)$ satisfy the state equations for $\alpha_n^1(kr)+\alpha_n^i$ and $\alpha_n^s(kr)$ given in [5] which should be solved subject to the boundary conditions

$$\alpha_n^s(kr_1)=F_n(k_1r_1)\alpha_n^1(kr_1)+\alpha_n^i \quad (15)$$

$$\alpha_n^1(kr_2)=0 \quad (16)$$

where the Mie scattering function $F_n(k_1r_1)$ is given by (6), but now

$$T_n=[r_1j_n(kr_1)]'j_n(k_1r_1)-\frac{j_n(kr_1)}{\epsilon_1}[r_1j_n(k_1r_1)]'. \quad (17)$$

The total field in the homogeneous inner core for $0\leqslant r\leqslant r_1$ is given by

$$E_r^c(r,\theta)=-Z_0(\epsilon_1)^{-1/2}\sum_{n=1}^{\infty}n(n+1)c_n\alpha_n^c j_n(k_1r)\frac{1}{k_1r}P_n \quad (18)$$

$$E_\theta^c(r,\theta)=-Z_0(\epsilon_1)^{-1/2}\sum_{n=1}^{\infty}c_n\alpha_n^c[rj_n(k_1r)]'\frac{1}{k_1r}\frac{d}{d\theta}P_n \quad (19)$$

where the multipole coefficient α_n^c is obtained from $E_\theta^c(r_1,\theta)=E_\theta^i(r_1,\theta)+E_\theta^{sc}(r_1,\theta)$ and the orthogonality of the Legendre's functions as

$$\alpha_n^c=\epsilon_1\{[\alpha_n^1(kr_1)+\alpha_n^i][r_1j_n(kr_1)]'+\alpha_n^s[rh_n^{(1)}(kr_1)]'\}/[r_1j_n(kr)]'. \quad (20)$$

The heating potential for the dipole excitation is given by $P_h=(1/2)\sigma(|E_r|^2+|E_\theta|^2)$, where E_r and E_θ are the spherical components of the total field and are given by $E_r=(\epsilon)^{-1}(E_r^i+E_r^{sc})$, $E_\theta=E_\theta^i+E_\theta^{sc}$ for the inhomogeneous layer and $E_r=E_r^c$, $E_\theta=E_\theta^c$ for the homogeneous inner core.

III. Numerical Results

The profiles shown in Fig. 2 correspond to those given by Shapiro *et al.* [1] at 3 GHz. The sinusoidal transitions between the layers can be made sharper or smoother by adjusting the values e_1,e_2,e_3 and d_1,d_2,d_3.

A computer program is developed which calculates the multipole coefficients of the scattered field for the problem illustrated in Fig. 1 and Fig. 2. The state equations are integrated by Hamming's modified predictor corrector method [8] for each n, and linear interpolation is applied to the scattering coefficients to find a close estimate of these coefficients at points where the heat potential is to be found. To make sure that the incident field, which is the near field of the loop or dipole antenna, is found correctly, these fields are also calculated by numerical integration for the loop antenna and from the analytical expression [7] for the dipole antenna. For the comparison $ka=0.3$, $kh=\pi/2$, and d (6.3 and 13 cm) are taken for the antennas and the electric field is computed at θ (30 and 90°) and r (0.159 and 3.3 cm). In the expansions (1), (10), and (11), $n_{\max}=N=11$ terms are used. It is found that the multipole expansions calculate the incident fields correctly up to four significant digits. The computer program calculating the multipole coefficients and, hence, the scattered fields is also checked by solving a homogeneous sphere as an inhomogeneously coated sphere by the present formulation and comparing the results with those obtained from the analytical Mie formulation [6] for both loop and dipole antenna excitations. A very good agreement is obtained between the two results. Table I presents the results of the comparison for the loop antenna excitation. The convergence of the spherical wave expansions used slows down as the complex dielectric constant and

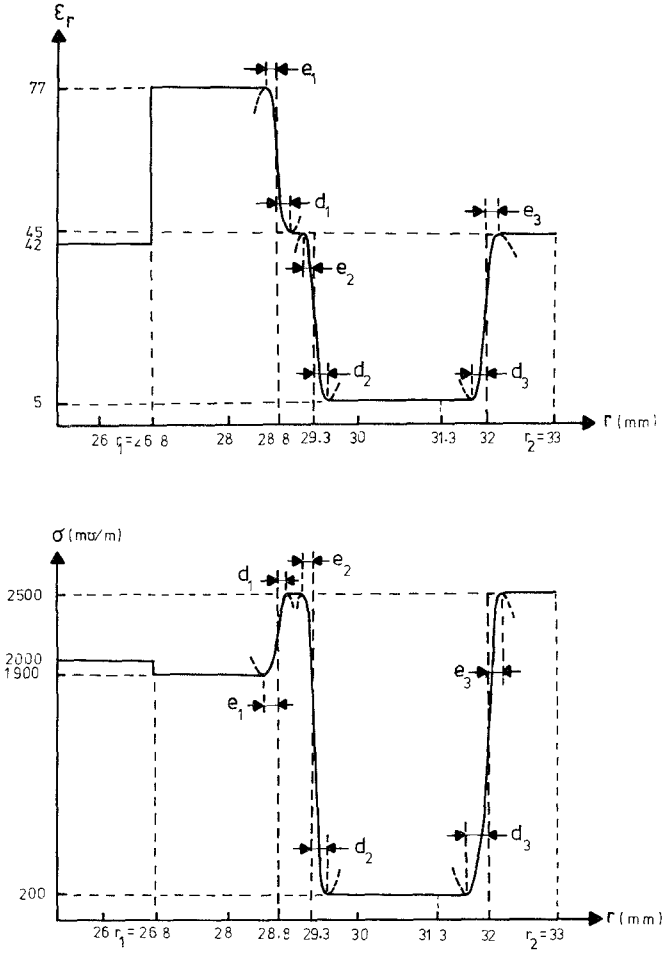

Fig. 2. The variation of the dielectric constant and conductivity with radius in Fig. 1.

TABLE I
HEAT POTENTIAL DISTRIBUTION (W/m³) IN A HOMOGENEOUS SPHERE EXCITED BY A SMALL LOOP ANTENNA ($r_1=2.68$ cm, $r_2=3.3$ cm, $\theta=90°$, $ka=0.3$, $f=3$ GHz, $I_0=1$ μA, $\epsilon_r=42$, $\sigma=2$ mho/m, $N=11$)

r(cm)	As coated sphere by present formulation	As homogeneous sphere by Mie formulation	d(cm)
0 0318	0 12206x10^{-11}	0.12217x10^{-11}	
1 3559	0 16698x10^{-9}	0 16700x10^{-9}	
2 6800	0.43830x10^{-10}	0 43848x10^{-10}	6 3
2 9900	0.46984x10^{-10}	0.47184x10^{-10}	
3.3000	0 50617x10^{-10}	0 51208x10^{-10}	
0.0318	0 80916x10^{-13}	0 80939x10^{-13}	
1.3559	0.12627x10^{-10}	0 12632x10^{-10}	
2 6800	0 80832x10^{-11}	0 80867x10^{-11}	12.3
2 9900	0 92661x10^{-11}	0 93026x10^{-11}	
3 3000	0 97570x10^{-11}	0.98183x10^{-11}	

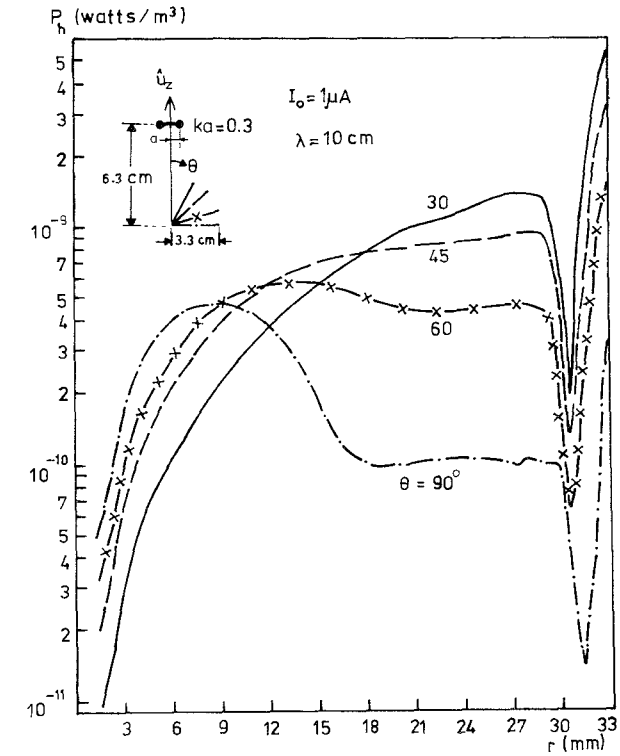

Fig. 3. Distributions of heat potential due to loop at $d=6.3$ cm.

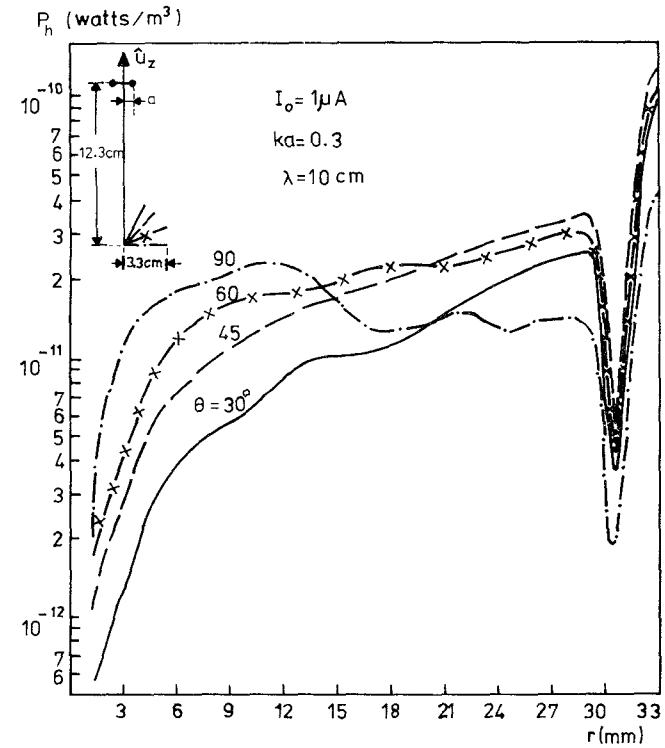

Fig. 4. Distributions of heat potential due to loop at $d=12.3$ cm.

the optical radius (kr_2) increase and the radial separation of the antenna and the field point decrease. In the present applications it is found that, with $N=9$ and 11 coefficients, the expansions converged satisfactorily. The computer time required increases with N, the thickness of the inhomogeneous layer, and the slope of the variation of the complex dielectric constant. Table I is produced in 20 min using double precision arithmetic in an IBM-370/145 system.

The heat potentials (P_h) are shown in Figs. 3–5 for the loop excitations and in Figs. 6–8 for the dipole excitations.

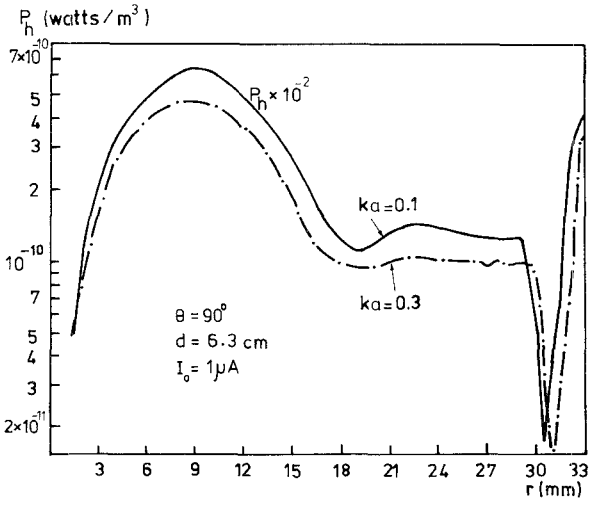

Fig. 5. Comparison of distributions of heat potential for two different loop radii.

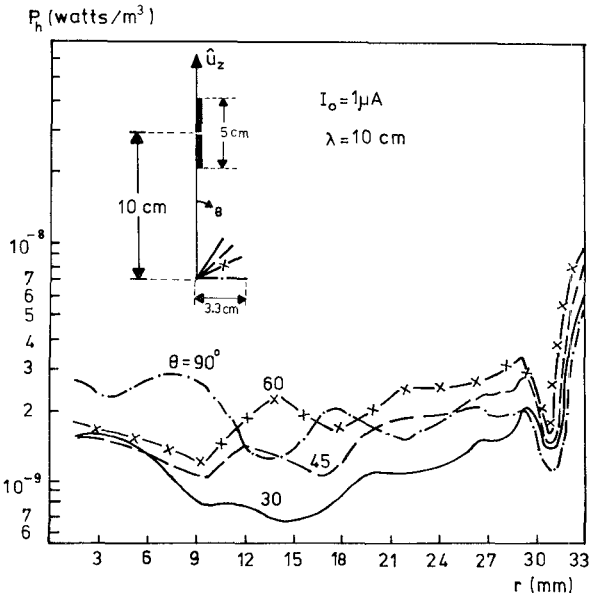

Fig. 6. Distributions of heat potential due to a half-wave dipole at $d=10$ cm.

For the loop excitations, heating the exact center of the sphere is not possible, as the loop does not radiate in the direction of its axis. However, a peak is observed close to the origin in the $\theta=90°$ plane. Increasing the distance of the loop to the sphere decreases the peak. The dip in the heat potential in the vicinity of the 31-mm radius is obviously due to the small conductivity of the bone and fat layers. It is seen that this dip shifts slightly with the radius of the loop. The results shown are for $e_1=2.0$ mm, $d_1=e_2=2.5$ mm, $d_2=d_3=1.35$ mm, and $e_3=0.97$ mm. When the values $e_1=0.955$ mm, $d_1=e_2=0.192$ mm, $d_2=d_3=0.675$ mm, and $e_3=0.478$ mm are used for sharper transitions between the layers, the results did not change significantly except that the dip around the 31-mm radius raised up slightly.

For the dipole excitation, the heat potential shows undulations with a more uniform distribution compared to

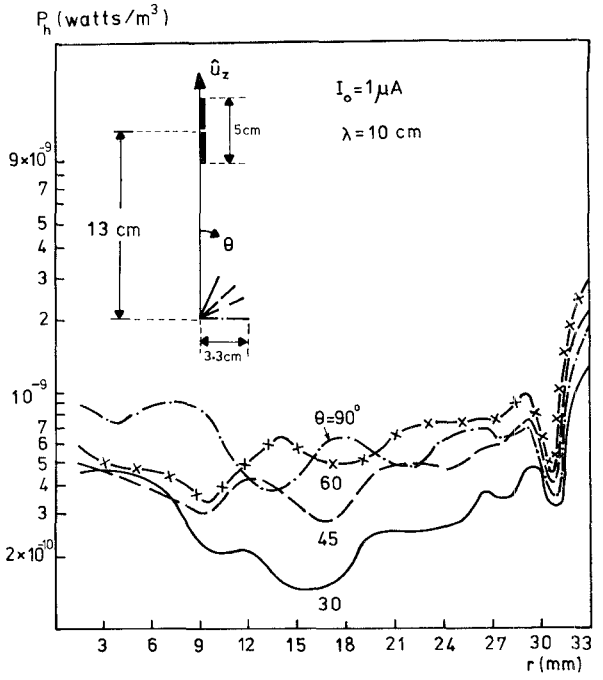

Fig. 7. Distributions of heat potential due to a half-wave dipole at $d=13$ cm.

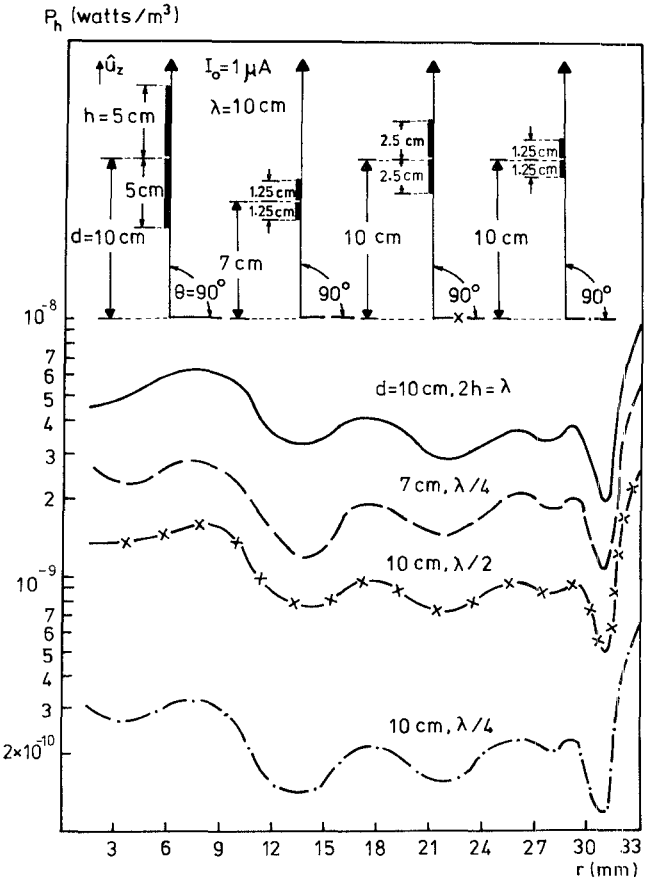

Fig. 8. Comparison of distributions of heat potential due to various dipole excitations.

the loop excitation. The effect of the distance of the dipole to the sphere and the length of the dipole (Figs. 7 and 8) on the heat potential seems to be only to change the level

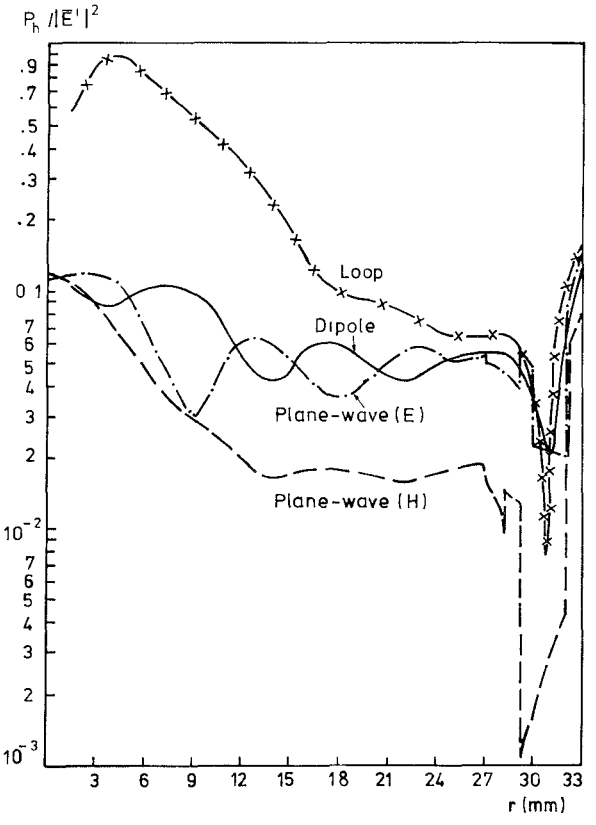

Fig. 9. Comparison of incident field normalized heat potentials at $\theta = 90°$ for loop antenna, dipole antenna, and plane-wave excitations.

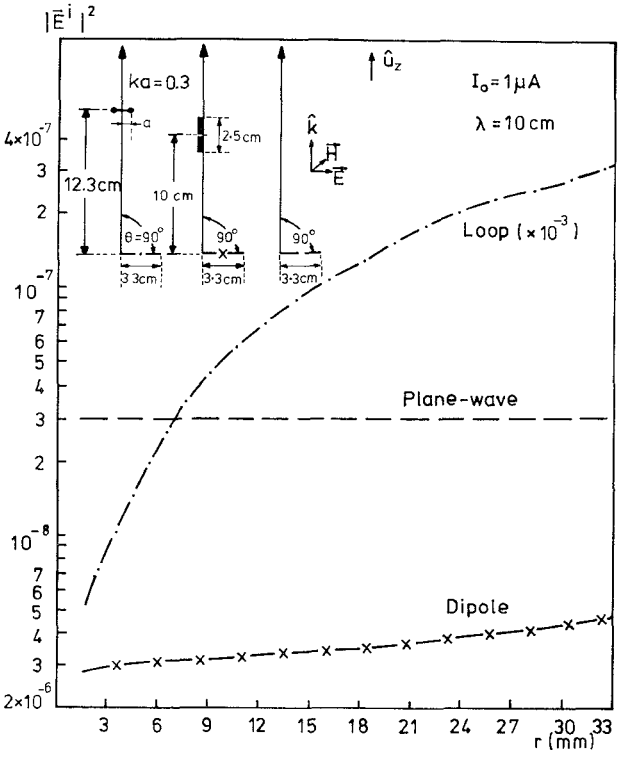

Fig. 10. Comparison of mean-squared incident powers at $\theta = 90°$.

of the variations. The smoother and the sharper transitions did not make any significant change in the results.

The results for plane-wave excitations are obtained from the literature [1] for comparison and given in Fig. 9. These results correspond to profiles with abrupt transitions, and the heat potential is normalized with the mean-squared incident power. For comparison, the curves at $\theta = 90°$ for loop and dipole excitations are normalized by the near-field mean-squared incident powers (Fig. 10) and also given in Fig. 9. It is seen that a similarity exists between the normalized heat potential for the plane-wave excitation in the direction of the incident electric field and the dipole excitation at $\theta = 90°$. For the case of the loop, both the incident power and the normalized heat potential show a large variation towards the center of the brain.

IV. Conclusion

Multilayered and inhomogeneous spherical models of a cranial structure of 33-mm radius at 3 GHz are rather an idealized model of a real physical structure. Nevertheless, the numerical results could have some relevance to the actual case.

It is seen that no considerable hot spots occur for the dipole excitation and a rather uniform heat potential distribution occurs. On the other hand, a hot spot is observed close to the origin for the loop antenna excitation at $\theta = 90°$. When compared with the plane-wave excitation, it is seen that the exact center of the head can best be heated by the plane-wave incidence. Also, for all excitations, a concentration of heat at this frequency and size can be observed at the skin because of the high conductivity of this outermost layer.

References

[1] A. R. Shapiro, R. F. Lutomirski, and H. T. Yura, "Induced fields and heating within a cranial structure irradiated by an electromagnetic plane wave," *IEEE Trans. Microwave Theory Tech.*, vol. MTT-19, pp. 187–196, Feb. 1971.

[2] C. M. Weil, "Absorption characteristics of multilayered sphere models exposed to UHF/microwave radiation," *IEEE Trans. Biomed. Eng.*, vol. BME-22, pp. 468–476, Nov. 1975.

[3] A. W. Guy, "Electromagnetic fields and relative heating patterns due to a rectangular aperture source in direct contact with bilayered biological tissue," *IEEE Trans. Microwave Theory Tech.* (*Special Issue on Biological Effects of Microwaves*), vol. MTT-19, pp. 214–223, Feb. 1971.

[4] H. S. Ho, "Contrast of dose distributions in phantom heads due to aperture and plane wave sources," *Ann. N.Y. Acad. Sci.*, vol. 247, pp. 454–472, 1975.

[5] A. Hizal and H. Tosun, "State-space formulation of scattering with application to spherically symmetrical objects," *Can. J. Phys.*, vol. 51, no. 5, pp. 549–558, 1973.

[6] J. A. Stratton, *Electromagnetic Theory*. New York: McGraw-Hill, 1941.

[7] R. Mittra, *Computer Techniques for Electromagnetics*. New York: Pergamon, 1973.

[8] R. W. Hamming, *Numerical Methods for Scientists and Engineers*. New York: McGraw-Hill, 1962, pp. 393–426.